Free Deposition Printing for Space Truss Structures

Romain Duballet, Romain Mesnil, Nicolas Ducoulombier, Paul Carneau, Leo Demont, Mahan Motamedi, Olivier Baverel, Jean-François Caron, Justin Dirrenberger

Free deposition printing for space truss structures *

Romain Duballet[1,2], Romain Mesnil[1], Nicolas Ducoulombier[1], Paul Carneau[1], Leo Demont[1], Mahan Motamedi[1], Olivier Baverel[1], Jean-François Caron[1], and Justin Dirrenberger[3]

[1] Laboratoire Navier, UMR 8205, Ecole des Ponts, CNRS, UGE, Champs-sur-Marne, France
romain.duballet@enpc.fr
[2] XTreeE, Le Manille, 18-20, rue du Jura, CP 40502, 94623 Rungis, France
[3] Laboratoire PIMM, Arts et Métiers, CNRS, Cnam,Paris, France

Abstract. This paper proposes a specific extrusion method for 3D printing of mortar called free deposition by the authors. It consists in letting a fine mortar flow through a moving nozzle above a support, here EPS foam. The aim is to obtain a regular lace, thus to avoid instability phenomena like coiling, and ensure a regular diameter, without stretching the lace. A rheological characterisation is proposed and is experimentally tested. This work takes place in the context of the building of space trusses in 3D printed concrete thanks to progressively assembled EPS foam blocks acting as support.

Keywords: Digital Fabrication · concrete printing

1 Introduction

This work deals with the prototyping of space truss structures in printed mortar, involving the assembly of EPS blocks as printing support. This building system has been described in [5] as a masonry concept, see Figure 1. Once assembled the blocks also protect the curing mortar. The mortar being printed on the blocks, it progressively acquire mechanical strength and can bear its own weight as well as the additional matter above. Yet the blocks support the printing, reducing the need for early age resistance for the mortar.

As such, the printing method differs from the usual concrete printing and can be called free deposition. The other three main printing approaches for extrusion based printing are slip-forming, lace shaping and lace pressing, see Figure 2 and [6]. Lace shaping relies on the extrusion of a mortar with a yield stress of 1000 Pa that has not to deform. Lace pressing uses admixtures to perform a phase change at the extrusion time and therefore can allow extrusion with early age yield stress of 100 Pa. The pressing relies on the material plasticity to ensure good layer adherence.

* Supported by LafargeHolcim and by the Build'in platform.

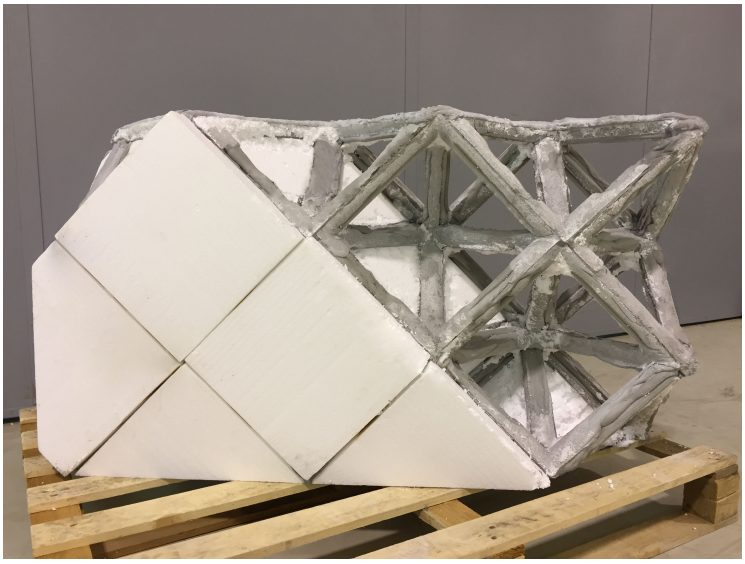

Fig. 1. Space Truss Masonry Wall with Robotic Extrusion, published in [5]

In the same spirit, free deposition works at low yield stress values at extrusion time to take advantage of mortar deformation in the support. The objectives are to ensure a correct quantity of deposited material, and a correct shape. Lace stretching and coiling must be avoided, therefore, specific deposition regimes are designed depending on the support slope angle, extrusion speed and flow rate, see section 2.

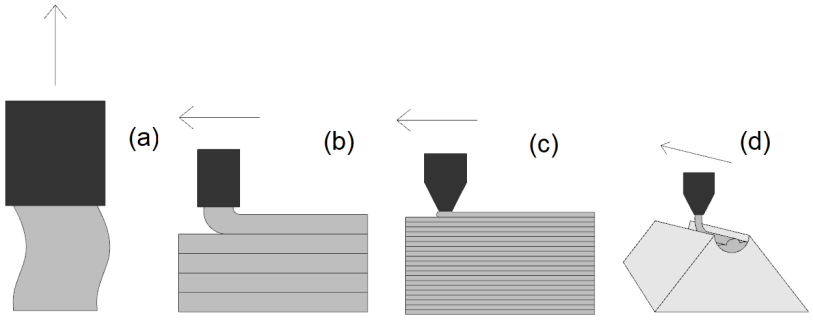

Fig. 2. The four main printing strategies : (a) Slip forming, (b) Extruded shaping, (c) Oriented pressing and (d) Free depositing, published in [6]

2 Process requirements

2.1 Notations

In the followings of this section, we consider a lace of height h, deposited from a height $H > h$ by an extruder with a circular nozzle of diameter d. The extrusion speed v_e (related to the flow rate Q by $Q = \rho g V_e \pi d^2/4$) and robot speed V_r are selected so that $V_e = V_r$ in most of the process, to avoid stretching of the lace. Since no stretching is involved, its is clear that the conservation of mass implies that $d = h$. The main geometrical parameters are represented in Figure 3. The application studied in this article involves slanted supported, with an inclination θ.

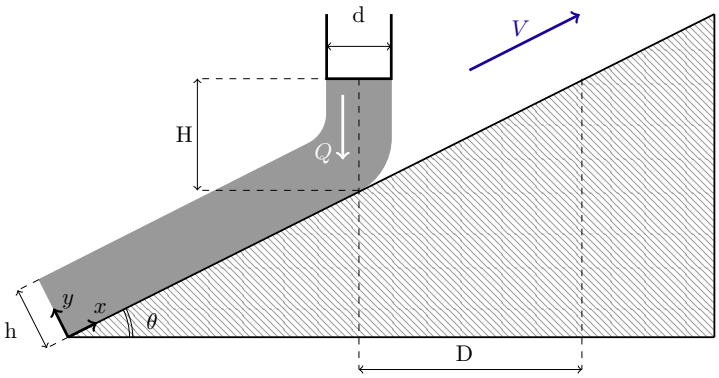

Fig. 3. Notations of the free-flow deposition

2.2 Rheological requirements

The proposed process is based on the extrusion of yield-stress fluid on slanted supports. The rheological requirements for the extruded material slightly differ from what is usually expected in typical 3d printing applications. In particular, the lace inclination induces a significant shear stress. The maximal stress $\underline{\underline{\sigma}}$ in one lace at simply defined by equation (1) (the x and y axes are represented in Figure 3).

$$\underline{\underline{\sigma}} = \rho g h \begin{pmatrix} \cos\theta \sin\theta & 0 \\ \sin\theta & 0 & 0 \\ 0 & 0 & 0 \end{pmatrix} \tag{1}$$

The component σ_{xx} corresponds to the weight of the lace, whereas $\sigma_{xy} = \sigma_{yx}$ is a shear stress due to the slope inclination. The yield stress τ_c can be compared to the Von Mises stress τ, which is computed in equation (2).

$$\tau(\theta) = \rho g h \sqrt{1 + 2\sin^2\theta} \tag{2}$$

The flow is initiated when the shear stress exceeds the material yield strength τ_c, This classically yields an avalanche phenomenon that what experimentally observed : the initiated flow yields a thinning of the lace and thus increases dynamic loading on the material below. From a practical point of view, it is thus preferable to keep the shear stress below the yield stress ($\tau(\theta) < \tau_c$). This imposes a constraint on the yield stress of the material described by equation (3).

$$\frac{\tau_c}{\rho g h} > \sqrt{1 + 2\sin^2\theta} \tag{3}$$

The case $\theta = 0$ is well-known in the literature and ensures that the lace is stable under its own self-weight. One can notice that the Von Mises criterion, classically used for yield stress fluids [4], seems to show that it is possible to print at any angle θ_c provided that the yield stress is high enough, this was explored by the authors [2] in a horizontal printing ($\theta_c = 90°$). In reality, the friction between the substrate and the lace might prevent to reach any arbitrary value of θ_c. For the latter case, a Mohr-Coulomb criterion with low cohesion could be applied to equation (1) without difficulty.

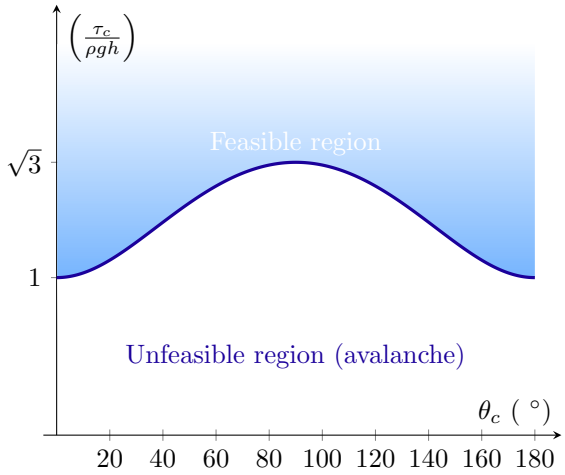

Fig. 4. Feasible domain for yield stress regarding the avalanche phenomenon

2.3 Deposition height

In the experiments presented in this paper, the nozzle remains aligned with the vertical axis. This brings a constraint on H, D and θ: $D \sim \frac{H}{\tan\theta}$. The nozzle should not collide with the printing bed, which implies that $D > h/2$. Finally, this brings an additional constraint on the minimal deposition height, as shown

in equation (4).

$$\begin{cases} \dfrac{H}{h} > 1 \ \ (\text{free} - \text{deposition}) \\ \dfrac{H}{h} > \dfrac{\tan\theta}{2} \ \ (\text{collision}) \end{cases} \tag{4}$$

The height is also constrained by a dripping phenomenon first described in [3] and revisited for mortar extrusion by some of the authors of this paper [7].The weight of the lace exerts a tensile force, which is maximal at the tip of the nozzle. When this tensile stress equals the yield stress, the material then rapidly detaches from the nozzle. The stress should thus remain inferior to the yield stress, in order to avoid jet instabilities and coiling. The critical height for this phenomenon is described by the following equation, first derived in [3]:

$$\frac{H}{h} < \frac{\sqrt{3}\tau_c}{\rho g h} \tag{5}$$

2.4 Coiling

The experimental data revealed a coiling phenomenon in several configurations, as as illustrated in Figure 5. Coiling of viscous threads is a well-known physical behaviour [10,1,11]: it is as an instability comparable to buckling (and occurs thus for $H/h > 1$, which is precisely the case of free deposition printing). When the rod is moving at a constant speed, this instability is triggered by the fact that the extrusion speed is superior to the robot speed ($V_r/V_e < 1$). The robot speed was calibrated so as to maintain $V_r/V_e = 1$, yet coiling occasionally occurred in our experiments. For more details on coiling, the reader is referred to [10], which identifies different coiling regimes. In the case of free deposition, stretching is negligible so that we encounter viscous coiling regime.

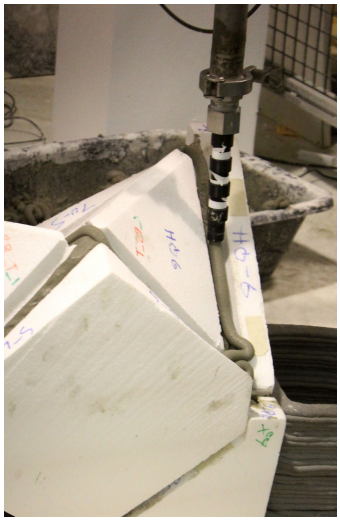

Fig. 5. Coiling pattern (meandering) at the bottom of the gutter.

It was experimentally observed that coiling occurred in the beginning of slopes when the robot is going up. There are two possible explanations. First, the interpolation of speeds is not perfect when abrupt direction changes are at stake, so that the robot speed can punctually differ from the extrusion speed (which is kept constant throughout the printing process). Second, the change between a constant speed horizontal $\mathbf{V_h}$ path and a constant speed inclined $\mathbf{V}_\theta$ path over a time period Δt implies that the nozzle and the mortar

in the extruder are subject to a vertical acceleration $V * \sin\theta/\Delta t$. The apparent gravity g' for the concrete is thus

$$g' = g + \frac{V \sin\theta}{\Delta t} \tag{6}$$

In practice, we have $V \sim 0.1m/s$, $\Delta t \sim 0.1s$, so that the acceleration can be of $1m.s^{-2}$. In our experimental set-up, the flow rate is controlled with a pump applying a pressure p to the fluid. The flow is controlled if $p > \rho g h$, or in the case $p > \rho g' h$. An increase of g' might thus lead to an overflow $Q+\delta Q$ in an otherwise well-calibrated process. Both explanations advocate for a better control of the robot speed in reorientation areas, in order to increase robotic accuracy and to decrease the dynamic loads applied to the fluid inside the printing head.

3 Experimental validation

A initial prototype with constant slope angle had been previously executed, see Figure 1 and [5]. For this work, a curved wall has been designed and fabricated for the sake of slope variation, see Figure 9.

3.1 Project description

The prototype is a curved space truss wall, standing on an overall surface of 1m x 3m and with a 1.8 meters height. The bars have a diameter of 4 cm and the total weight is of approximately 120 kg. The process constraints as well as performance metrics have been merged in a parametric model, see Figure 6.

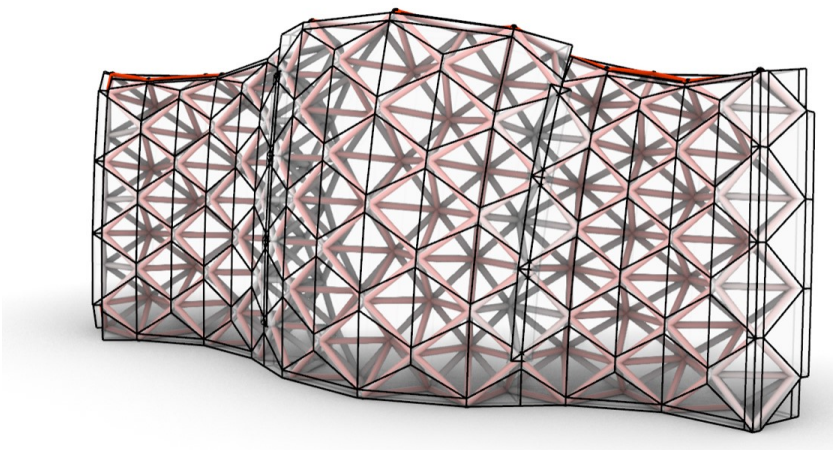

Fig. 6. Parametric design of the curved prototype

The curved tessellation has been obtained from the principal curvature lines of a cyclidic net generated thanks to the method described in [9]. Each block has a unique geometry and has been made by robotic hot-wire cutting, see Figure 7.

Fig. 7. Robotically hot-wire cut EPS blocks, cut at l'Ecole des Ponts ParisTech (picture: Romain Mesnil)

3.2 Rheological requirements

The extruded mortar is a bi-component material [8] with an initially low yield stress (around 100 Pa), an accelerator is added to increase the yield stress at the nozzle's tip. The nozzle diameter is $h = 15$mm, we consider that $\rho g \sim 24\text{kN/m}^3$. The maximal angle is $\theta_c \sim 60°$. The minimal yield stress required is found with equation (2) and yields $\tau_{c,min} \sim 550$Pa. The actual yield stress was measured in the beginning of the printing with the drip experiments described in [7] and is in accordance with this theoretical value.

3.3 Printing set-up

For this prototype the extrusion has been handled with an ABB 6620 robot and an XtreeE bi-component printing head, and the trajectories/speed mapping generated with HAL Robotics grasshopper plug-in. The EPS blocks were manually

placed between each macro layer (horizontal group of blocks), thus creating some precision issues. They were partially solved by calibrating the blocks positions with the robot.

The total lace length L_{lace} is different from the length of the trajectory of the nozzle L_{nozzle}, because the latter is above the blocks, and slope changes create incompatibilities between the lace and toolpath length. This is a practical issue, because free deposition relies on the deposition of an unstressed lace. The conservation of mass indicates that the robot velocity should be adapted so that for each section:

$$V_r L_{nozzle} = V_e L_{lace} \tag{7}$$

3.4 Discussion

On figure 8 we can see a correct deposition regime, happening on the bottom macro layers of the prototype. It validates the theoretical approach for free deposition on slope varying support. As the wall rose, imprecision due to manual placement of blocks increased, therefore resulting in deviation from theoretical position of the nozzle. This created some coiling issued, visible on figure 9. This was not visible on the first prototype (Figure 1) due to the constant slope angle and block 3D orientation.

Fig. 8. Free deposition on EPS blocks with correct regime (no coiling, no streching)

4 Conclusion and Perspectives

This article introduces a new extrusion process, called free deposition by the authors. Process requirements for this extrusion strategy are detailed. A prototype with varying support sizes and orientations has been produced.

Fig. 9. The completed truss, after removal of some EPS blocks (photo: Stefano Borghi).

This approach does not face the same difficulties as other concrete printing methods regarding the reinforcement issue. Layered printing indeed bring anisotropy to the objects it makes, and if reinforcement is to be added to the lace, it will not be possible to orient it in the perpendicular direction. This problem can perhaps be solved by playing with the extrusion path to somehow weave the laces to each other to recreate a global isotropy. In the truss case, the structure has a natural anisotropic behaviour since the forces are oriented along the bars. Lace reinforcement is therefore compatible in principle. Depending on the specific strategy though, some problems remain to be solved.

Among the various possibilities to deal with this generalized printing, layered free deposition of plastic mortar is compatible with the addition of rebars. Indeed, one could imagine, in the same way that the EPS blocks are progressively assembled, to put metallic sticks inside each bar, between the deposition of layers. Correct adherence with the mortar would have to be carefully checked, but does not seem impossible considering the relatively low demand in early age structuration. Fiber reinforcement of the lace is also compatible with such a method and is currently explored by the authors.

References

1. Brun, P.T., Audoly, B., Ribe, N.M., Eaves, T.S., Lister, J.R.: Liquid ropes: a geometrical model for thin viscous jet instabilities. Physical review letters **114**(17), 174501 (2015)
2. Carneau, P., Mesnil, R., Baverel, O., Roussel, N.: Additive manufacturing of cantilever - from masonry to concrete 3d printing. Automation in Construction (2020), under review
3. Coussot, P., Gaulard, F.: Gravity flow instability of viscoplastic materials: The ketchup drip. Phys. Rev. E **72**, 031409 (Sep 2005). https://doi.org/10.1103/PhysRevE.72.031409, `https://link.aps.org/doi/10.1103/PhysRevE.72.031409`
4. Coussot, P.: Rheometry of pastes, suspensions, and granular materials: applications in industry and environment. John Wiley & Sons (2005)
5. Duballet, R., Baverel, O., Dirrenberger, J.: Space truss masonry walls with robotic mortar extrusion. Structures **18**, 41 – 47 (2019). https://doi.org/https://doi.org/10.1016/j.istruc.2018.11.003, `http://www.sciencedirect.com/science/article/pii/S2352012418301309`, advanced Manufacturing and Materials for Innovative Structural Design
6. Duballet R., Baverel O., D.J.: Building systems in robotic extrusion of cementitious materials (2019), `https://www.researchgate.net/publication/337186115_Building_systems_in_robotic_extrusion_of_cementitious_materials/citations`
7. Ducoulombier, N., Carneau, P., Mesnil, R., Caron, J.F., Roussel, N.: "the slug test": Rheology and homogeneity assessment for robotic extrusion of yield stress fluid. Digital Concrete (2020), under review
8. Gosselin, C., Duballet, R., Roux, P., Gaudillière, N., Dirrenberger, J., Morel, P.: Large-scale 3D printing of ultra-high performance concrete – a new processing route for architects and builders. Materials & Design **100**, 102–109 (2016), `http://www.sciencedirect.com/science/article/pii/S0264127516303811`
9. Mesnil, R., Douthe, C., Baverel, O., Léger, B.: Morphogenesis of surfaces with planar lines of curvature and application to architectural design. Automation in Construction **95**, 129 – 141 (2018). https://doi.org/https://doi.org/10.1016/j.autcon.2018.08.007, `http://www.sciencedirect.com/science/article/pii/S0926580518301547`
10. Ribe, N.M.: Coiling of viscous jets. Proceedings of the Royal Society of London. Series A: Mathematical, Physical and Engineering Sciences **460**(2051), 3223–3239 (2004). https://doi.org/https://doi.org/10.1098/rspa.2004.1353
11. Yuk, H., Zhao, X.: A new 3d printing strategy by harnessing deformation, instability, and fracture of viscoelastic inks. Advanced Materials **30**(6), 1704028 (2018). https://doi.org/10.1002/adma.201704028, `https://onlinelibrary.wiley.com/doi/abs/10.1002/adma.201704028`